Modelling spherical joints in multibody systems

Mariana R. Silva, Filipe Marques, Miguel T. Silva, Paulo Flores

Abstract. Spherical joints are commonly utilized in many real-world scenarios. From the more simplistic to the more complex perspectives, spherical joints might be modelled considering different cases. Thus, the aim of this study is to analyze and compare the influence of different spherical joint modelling approaches, namely the ideal, dry, lubricated, and bushing models, on the dynamic response of multibody systems. Initially, the kinematic and dynamic aspects of the spherical joint models are comprehensively reviewed. In this process, several approaches are explored and studied considering the normal, tangential, lubrication and bushing forces experienced by the multibody systems in such cases of spherical joints. The application of the spherical joint models in the dynamic modeling and simulation of the spatial four bar mechanism is investigated. From the results obtained, it can be stated that the choice of the spherical joint model can significantly affect the dynamic response of mechanical multibody systems.

Key words: Spherical joints, Dry joints, Lubricated joints, Bushing joints, Contact mechanics, Multibody dynamics

Mariana R. Silva
CMEMS-UMinho, Departamento de Engenharia Mecânica, Universidade do Minho, Campus de Azurém, Guimarães 4804-533, Portugal, e-mail: m.silva@dem.uminho.pt
Filipe Marques
CMEMS-UMinho, Departamento de Engenharia Mecânica, Universidade do Minho, Campus de Azurém, Guimarães 4804-533, Portugal, e-mail: fmarques@dem.uminho.pt
Miguel T. Silva
IDMEC, Instituto Superior Técnico, Universidade de Lisboa, Lisboa, Portugal, Av. Rovisco Pais, 1, Lisboa 1049-001, Portugal, e-mail: MiguelSilva@tecnico.ulisboa.pt
Paulo Flores
CMEMS-UMinho, Departamento de Engenharia Mecânica, Universidade do Minho, Campus de Azurém, Guimarães 4804-533, Portugal, e-mail: pflores@dem.uminho.pt

1 Introduction

Considering the type of applications in which they are designed to operate, spherical joints may be characterized using different models. The simplest approach is to consider the spherical joint as an ideal joint, that is, with no clearance between the socket and the ball. However, in many applications there is clearance between these components. In this case, the dynamics of the joint is controlled by contact-impact forces that develop on the ball and socket and that result from their collision. In multibody systems, instead of dealing with kinematic constraints as in the ideal joint, the spherical clearance joint deals with force constraints. The contact-impact forces developed can significantly affect the dynamic response of the system [3].

One of the most commonly utilized solutions to avoid or reduce the contact within dry clearance joints and to minimize the energy dissipation, is to add a lubricant fluid in the space between the socket and the ball, that is, in the clearance space. The high pressures that develop in this fluid act to keep the ball and the socket apart, preventing the contact between these two components [4, 5]. In other applications, bushing elements may be utilized. These are usually composed of elastomeric materials and are used to absorb shocks and vibrations, handle misalignments, reduce noise and wear, and decrease the transmissibility of irregularities to the system [1].

With this knowledge in perspective, the aim of this study is to analyze and compare the influence of different spherical joint models on the dynamic response of multibody systems. For this purpose, the kinematic and dynamic aspects of the ideal, dry, lubricated, and bushing models are presented. In the aftermath of this process, the spatial four bar mechanism is considered as a demonstrative example of application. This study provides a simple and direct comparison between different methodologies that can be applied to mechanical systems with spherical joints, allowing a better choice of the model to adopt for specific applications.

2 Kinematics of Spherical Joints

This section includes a description of the formulations utilized in multibody systems to model the kinematic aspects of spherical joints. Several cases are presented, namely the ideal, dry, lubricated, and bushing joint models.

Ideal spherical joints allow the relative rotations between two adjacent bodies i and j, constraining three relative translations. Consequently, the center of the ideal spherical joint has constant coordinates with respect to any of the local coordinate systems of the connected bodies. This means that point P_i on body i is coincident with point P_j on body j. Points P_i and P_j represent the center of the socket and ball, respectively [2]. The condition of the coincidence of points P_i and P_j is as follows:

$$\mathbf{\Phi}^{(s,3)} \equiv \mathbf{r}_j^P - \mathbf{r}_i^P = \mathbf{r}_j + \mathbf{s}_j^P - \mathbf{r}_i - \mathbf{s}_i^P = \mathbf{0} \tag{1}$$

where $\mathbf{r}_k^P$ represents the global position vector of point P located on body k, $\mathbf{r}_k$ denotes the position vector of the center of mass of body k described in global coor-

dinates and $\mathbf{s}_k^P$ is the global position vector of point P located on body k with respect to local coordinates.

The velocity constraint equations for an ideal spherical joint are obtained by taking the first time derivative of Eq. (1), and can be expressed as [2]:

$$\dot{\mathbf{\Phi}}^{(s,3)} = \dot{\mathbf{r}}_j + \dot{\mathbf{s}}_j^P - \dot{\mathbf{r}}_i - \dot{\mathbf{s}}_i^P = \mathbf{0} \tag{2}$$

in which the dot represents the derivative with respect to time.

Considering the following condition:

$$\dot{\mathbf{s}} = \tilde{\boldsymbol{\omega}}\mathbf{s} = -\tilde{\mathbf{s}}\boldsymbol{\omega} \tag{3}$$

where the symbol ~ represents the skew symmetric matrix and $\boldsymbol{\omega}$ is the angular velocity, then Eq. (2) can be rewritten as follows [2].

$$\dot{\mathbf{\Phi}}^{(s,3)} = \dot{\mathbf{r}}_j - \tilde{\mathbf{s}}_j^P\boldsymbol{\omega}_j - \dot{\mathbf{r}}_i + \tilde{\mathbf{s}}_i^P\boldsymbol{\omega}_i = \mathbf{0} \tag{4}$$

In this sense, the time derivative of Eq. (4) yields the acceleration constraint equations of the ideal spherical joint as follows [2]:

$$\ddot{\mathbf{\Phi}}^{(s,3)} = \ddot{\mathbf{r}}_j - \tilde{\dot{\mathbf{s}}}_j^P\boldsymbol{\omega}_j - \tilde{\mathbf{s}}_j^P\dot{\boldsymbol{\omega}}_j - \ddot{\mathbf{r}}_i + \tilde{\dot{\mathbf{s}}}_i^P\boldsymbol{\omega}_i + \tilde{\mathbf{s}}_i^P\dot{\boldsymbol{\omega}}_i = \mathbf{0} \tag{5}$$

The multibody formulation for the case of ideal spherical joints was presented. However, in real-world application scenarios spherical joints present some level of clearance between the socket and the ball. The condition of coincidence between point P_i and point P_j assumed for the ideal joint case is disregarded in the case of the spherical clearance joint. Thus, the three kinematic constraints shown in Eq. (1) are removed and the two bodies are separated and free to move relative to one another. Contrary to the ideal joint case, the spherical clearance joint does not constrain any degree of freedom from the system [4, 5].

In a spherical clearance joint, a spherical part of body j, the ball, resides inside a spherical part of body i, the socket. The radii of the socket and the ball are R_i and R_j, respectively, and the difference between these parameters defines the size of the radial clearance as [4, 5]:

$$c = R_i - R_j \tag{6}$$

The vector connecting point P_i to point P_j is defined as the eccentricity vector, $\mathbf{e}$, which is obtained as :

$$\mathbf{e} = \mathbf{r}_j^P - \mathbf{r}_i^P \tag{7}$$

The magnitude of the eccentricity vector is given by:

$$e = \sqrt{\mathbf{e}^{\mathrm{T}}\mathbf{e}} \tag{8}$$

and the time rate of change of the eccentricity in the radial direction, that is, in the direction of the line of centers of the socket and the ball, is written as follows:

$$\dot{e} = \frac{\mathbf{e}^{\mathrm{T}}\dot{\mathbf{e}}}{e} \tag{9}$$

In spherical clearance joints, the situation in which the socket and the ball are contacting with each other is identified by a relative pseudo-penetration δ. The geometric condition for contact between the socket and the ball is defined as:

$$\delta = e - c \tag{10}$$

and the relative normal contact velocity, $\dot{\delta}$, is given by:

$$\dot{\delta} = \left(\dot{\mathbf{r}}_j^Q - \dot{\mathbf{r}}_i^Q\right)^{\mathrm{T}} \frac{\mathbf{e}}{e} \tag{11}$$

where Q_i and Q_j are the contact points on bodies i and j.

When the clearance joints are considered dry, normal and friction forces are the only effects present when physical contact is detected between the surfaces. However, in most mechanisms and machines, the joints are designed to operate with some lubricant fluid with the purpose of ensuring better performance of the mechanical systems by reducing friction and wear, providing load-carrying capacity, and adding damping to dissipate undesirable vibrations [4, 5]. In the case of a spherical joint with lubrication, the space between the ball and the socket is filled with a lubricant. Under applied load, the ball center is displaced from the socket center and the lubricant is forced into the clearance space, provoking a buildup of pressure. The high pressures generated in this lubricant film act to keep the bodies apart. Lubricated joints are designed so that, even when the maximal load is applied, the socket and the ball do not come in contact [5].

Bushing elements are utilized in many mechanical systems to absorb shocks and vibrations, handle misalignments and decrease the transmissibility of irregularities to the system [1]. The formulation utilized in this study closely follows the methodology presented by Ambrósio and Veríssimo [1], in which the bushing element is modelled in the multibody code as a nonlinear restrain that relates the relative displacements between the bodies connected with the joint reaction forces.

The kinematic aspects of spherical clearance joints with lubrication and with bushing elements are similar to those of the dry spherical joint.

3 Dynamics of Spherical Joints

This section includes a description of the formulations utilized in multibody systems to model the dynamics of spherical joints. The normal, tangential, lubrication and bushing force models are presented. These forces are introduced in the equations of motion of a multibody system as external generalized forces.

In the case of the dry spherical clearance model, the dynamics of the joint is controlled by contact-impact forces arising from the collision between the connected bodies. This type of joint can, thus, be referred to as force joint, since it deals with force effects rather than kinematic constraints [4, 5].

Within the scope of this study, the model developed by Lankarani and Nikravesh [6] is analyzed. The authors proposed a continuous contact force model for the contact-impact analysis of multibody systems using the general trend of Hertz contact law incorporated with a hysteresis damping factor to include energy dissipation in terms of internal damping. The contact force model is expressed as:

$$f_{\mathrm{n}} = K\delta^{n}\left[1+\frac{3(1-c_{\mathrm{r}}^{2})}{4}\frac{\dot{\delta}}{\dot{\delta}^{(-)}}\right] \tag{12}$$

where K denotes the generalized stiffness parameter, δ is calculated by Eq. (10), n represents the nonlinear exponent factor, c_{r} is the restitution coefficient, $\dot{\delta}^{(-)}$ denotes the initial contact velocity and $\dot{\delta}$ is obtained from Eq. (11).

In real-world applications of mechanical systems involving contacting surfaces with relative motion, friction forces of complex nature might arise. Thus, a rigor-

ous evaluation of these forces is warranted to obtain an accurate modelling of the dynamic response of the system. In the model proposed by Threlfall [7], the friction force and velocity are related by an exponential function whose purpose is to address the numerical difficulties associated with the discontinuity in Coulomb's law. The model was the basis for other friction force models, such as the continuous function expressed as:

$$\mathbf{f}_t = f_c \tanh\left(\frac{v_t}{v_1}\right)\frac{\mathbf{v}_t}{v_t} \tag{13}$$

where $\mathbf{v}_t$ is the tangential velocity of the contact point, v_t denotes the magnitude of the tangential velocity, v_1 represents the tolerance for the velocity and f_c is the magnitude of the Coulomb friction represented as follows:

$$f_c = \mu_k f_n \tag{14}$$

in which μ_k is the kinetic coefficient of friction and f_n is the normal contact force.

Concerning lubricated spherical joints, the squeeze-film and the wedge-film actions comprise the two main groups in which these joints can be categorized into. The squeeze-film action is associated with situations in which the ball does not rotate significantly about is center, but instead it moves along some path inside the socket boundaries. The wedge-film action refers to situations in which the ball has significant rotation, which this is usually observed in high-speed rotating machinery [5]. In this study, the squeeze-film action is considered.

The lubrication force due to squeeze-film action developed between the socket and the ball when there is lubricant fluid between these two components can be modelled using a law developed by Flores and Lankarani [2] as follows:

$$f_l = \frac{6\pi\nu\dot{e}R_j}{(c/R_j)^3}\left[\frac{1}{\varepsilon^3}\ln(1-\varepsilon)+\frac{1}{\varepsilon^2(1-\varepsilon)}-\frac{1}{2\varepsilon}\right] \tag{15}$$

where ν represents the dynamic lubricant viscosity, $\dot{e}$ is given by Eq. (9), and ε denotes the eccentricity ratio given by:

$$\varepsilon = \frac{e}{c} \tag{16}$$

where c and e are given by Eqs. (6) and (8), respectively.

For nonideal spherical joints, vector **e** given by Eq. (7) can be characterized as the gap between the ball and the socket. However, this vector can be defined as the deformation of the elastomer in a spherical joint with a bushing element [1]. Considering this statement, the force due to the bushing deformation adopted in this study is based on the formulation developed by Ambrósio and Veríssimo [1], and it is represented by the following condition:

$$\mathbf{f}_b = \left[k\left(\delta + b\dot{\delta}\right)\right]\frac{\mathbf{e}}{e} \tag{17}$$

where k is the stiffness of the bushing element, δ denotes the bushing deformation and b represents the stiffness proportional damping parameter.

As previously determined, the length of vector **e** is given by Eq. (8). Assuming that no gap exists between the bushing element and the ball, then $e=\delta$ and, thus, the time derivative of δ is given by Eq. (9).

4 Demonstrative Example of Application

The objective of this section is to examine the influence of the different cases for modelling spherical joints on the dynamic response and behavior of multibody systems. To this end, a spatial four-bar mechanism is utilized.

The spatial four-bar mechanism is composed by four rigid bodies, namely the ground, crank, coupler, and rocker. The numbers of each body and their corresponding local coordinate systems are shown in Fig. 1.

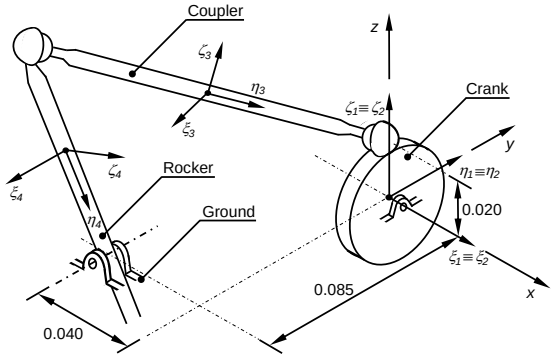

Fig. 1 Schematic representation of the spatial four-bar mechanism

The bodies of the spatial four bar mechanism are kinematically connected to each other by means of two revolute joints, connecting the ground to the crank and the ground to the rocker, and two spherical joints, connecting the crank to the coupler and the coupler to the rocker. Clearance and bushing are introduced in the spherical joint connecting the coupler and the rocker to analyze the dry, lubricated, and bushing models. The remaining joints are considered ideal.

The initial configuration of the spatial four-bar mechanism is presented in Fig. 1 and the corresponding initial values are presented in Table 1. The system is released from the initial position with null velocities and under the action of gravitational force, acting on the negative z-direction. For the nonideal joint models, initially the ball and the socket of the spherical clearance joint are concentric.

Table 1 Initial configuration of the spatial four-bar mechanism

Body Nr.	x [m]	y [m]	z [m]	e_0	e_1	e_2	e_3
2	0.00000	0.00000	0.00000	1.0000	0.0000	0.0000	0.0000
3	-0.03746	-0.04250	0.04262	0.9186	-0.1764	0.06747	-0.3472
4	-0.05746	-0.08500	0.03262	0.3634	-0.6066	-0.6066	0.3634

The dimensions and inertial properties of each body of the spatial four bar mechanism are presented in Table 2.

Table 2 Dimensions and inertial properties of the spatial four-bar mechanism

Body Nr.	Length [m]	Mass [kg]	Moment of inertia [kgm^2]		
			$I_{\xi\xi}$	$I_{\eta\eta}$	$I_{\zeta\zeta}$
2	0.020	0.0196	0.0000392	0.0000197	0.0000197
3	0.122	0.1416	0.0017743	0.0000351	0.0017743
4	0.074	0.0316	0.0001456	0.0000029	0.0001456

The simulation parameters used in all dynamic simulations and in the numerical methods required to solve the dynamics of the system are displayed in Table 3.

Table 3 Common and specific simulation parameters for the four-bar mechanism

Common			
Baumgarte coefficient, α	5	Reporting time step	0.00001s
Baumgarte coefficient, β	5	Integration tolerance	10^{-10}
Integrator algorithm	ode15s	Simulation time	2 s
Dry Model			
Young's modulus, E	207 GPa	Velocity tolerance, v_l	0.0010
Poisson's ratio, ν	0.3	Kinetic coefficient of friction, μ_k	0.1
Nonlinear exponent, n	1.5	Socket radius, R_i	10 mm
Restitution Coefficient, c_r	0.9	Ball radius, R_j	9.9 mm
Lubricated Model			
Dynamic lubricant viscosity, ν – 400 cP			
Bushing Model			
Bushing stiffness, k - 2.146×10^7 N/m		Stiffness proportional damping, b - 0.01	

The results obtained for the spherical joint models studied are shown in Fig. 2.

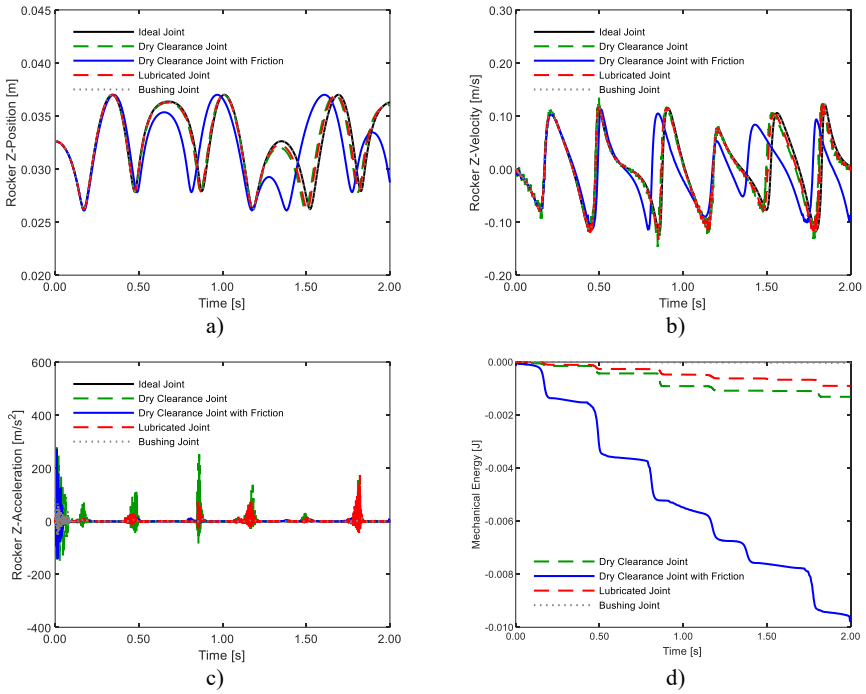

Fig. 2 Influence of the spherical joint model on the response of the spatial four-bar mechanism. a) Position, b) velocity, c) acceleration of the rocker and d) mechanical energy of the system.

It can be observed that the dynamic performance of the four-bar mechanism is significantly affected by the model chosen to characterize the spherical joint. In general, the frictionless joint model, exhibits more oscillations and produces significantly larger velocities and accelerations than the other models, suggesting that

the response of the system becomes chaotic. In fact, the addition of friction to the dry spherical clearance joint tends to smooth the behavior of the system, leading to a less chaotic behavior. The observation of Fig. 2 (c) also indicates that the spatial four-bar mechanism produces significantly lower accelerations with the ideal joint model when compared to the other models. Concerning the variation of the mechanical energy, the model with friction presents higher energy dissipation, followed by the frictionless and lubricated models, as observed in Fig. 2 (d). As expected, the bushing model produces positions, velocities and accelerations close to the ideal joint case, which means that the bushing element is, in fact, decreasing the noise associated with clearance and stabilizing the system, making it less chaotic. This model dissipates the least amount of energy comparing to the others.

5 Conclusions

The dynamic modeling and analysis of spatial mechanisms with different models for spherical joints has been presented in this work. The main kinematic and dynamic aspects related to these models were described under the framework of multibody systems methodologies. A classic spatial four bar mechanism was considered as a demonstrative application example to study the effect of the joint modeling approaches. Overall, the joint models strongly affect the performance of the system, essentially visible in terms of accelerations and mechanical energy.

Acknowledgments This work has been supported by Portuguese Foundation for Science and Technology, under the national support to R&D units grant, with the reference project UIDB/04436/2020 and UIDP/04436/2020, as well as through IDMEC, under LAETA, project UIDB/50022/2020.

References

1. Ambrósio, J., Verissimo, P.: Improved bushing models for general multibody systems and vehicle dynamics. *Multibody System Dynamics*. **22**, 341–365 (2009). https://doi.org/10.1007/s11044-009-9161-7
2. Flores, P.: Concepts and Formulations for Spatial Multibody Dynamics. Springer International Publishing (2015)
3. Flores, P., Ambrósio, J., Pimenta Claro, J. C., Lankarani, H.M.: Dynamics of Multibody Systems with Spherical Clearance Joints. *ASME Journal of Computational and Nonlinear Dynamics*. **1**, 240–247 (2006). https://doi.org/10.1115/1.2198877
4. Flores, P., Ambrósio, P., Pimenta Claro, J.C., Lankarani, H.M.: Kinematics and Dynamics of Multibody Systems with Imperfect Joints - Models and Case Studies. Springer-Verlag Berlin Heidelberg (2008)
5. Flores, P., Lankarani, H.M.: Spatial rigid-multibody systems with lubricated spherical clearance joints: modeling and simulation. *Nonlinear Dynamics* **60**, 99–114 (2010). https://doi.org/10.1007/s11071-009-9583-z
6. Lankarani, H.M., Nikravesh, P.E.: A Contact Force Model with Hysteresis Damping for Impact Analysis of Multibody Systems. *Journal of Mechanical Design* **112**, 369–376 (1990). https://doi.org/10.1115/1.2912617
7. Threlfall, D.C.: The inclusion of Coulomb friction in mechanisms programs with particular reference to DRAM au programme DRAM. *Mechanism and Machine Theory* **13**, 475–483 (1978). https://doi.org/https://doi.org/10.1016/0094-114X(78)90020-4